



|                    |   |
|--------------------|---|
| <b>Title</b>       | <b>Cyclic behaviour of connecting beams in reinforced concrete slit shear walls</b>                               |
| <b>Author(s)</b>   | <b>Kwan, AKH; Cheung, YK; Lu, XL</b>  |
| <b>Citation</b>    | <b>Proceedings Of The Institution Of Civil Engineers: Structures And Buildings, 1994, v. 104 n. 3, p. 317-324</b> |
| <b>Issued Date</b> | <b>1994</b>   |
| <b>URL</b>         | <b><a href="http://hdl.handle.net/10722/70831">http://hdl.handle.net/10722/70831</a></b>                          |
| <b>Rights</b>      | <b>Creative Commons: Attribution 3.0 Hong Kong License</b>  |

# Cyclic behaviour of connecting beams in reinforced concrete slit shear walls

A. K. H. Kwan, BSc(Eng), PhD, MICE, Y. K. Cheung, DSc, DE, FEng,  
and X. L. Lu, BSc(Eng), PhD

■ **The connecting beams in slit shear walls are generally much shorter than those in ordinary coupled shear walls and may therefore behave quite differently. In order to investigate the shear behaviour of such short connecting beams, two series of shear tests, one on monotonic behaviour and the other on cyclic behaviour, were carried out. Altogether, 24 specimens were tested. The results of the monotonic shear tests have been reported in an earlier paper. This Paper presents some additional information on the ductility of the beams as revealed by the monotonic shear tests, and the results of the cyclic shear tests. From the cyclic shear tests, the cracking and failure characteristics, reinforcement stress distribution, stiffness and strength degradations, ductility and damping capacity, etc., of the connecting beams are studied. The results are useful for evaluating the seismic performance of reinforced concrete slit shear walls.**

## Notation

$A_h$  area within hysteresis loop  
 $A_s$  area under skeleton curve  
 $\zeta$  damping ratio

## Introduction

In two earlier papers,<sup>1,2</sup> the Authors proposed the slit shear wall system as a new breed of earthquake resistant structure. Basically, a slit shear wall (Fig. 1) is a shear wall structure with vertical slits purposely cast within the wall panel and may be regarded as a pair of coupled shear walls with very short connecting beams. Under normal loading conditions, the connecting beams remain elastic so that the slit shear wall acts like a solid shear wall, but when affected by a strong earthquake, the connecting beams will first crack and yield and then serve as damping devices to dissipate the excessive seismic energy. It is hoped that by transforming the solid shear wall into a coupled shear wall structure through the introduction of vertical slits, the seismic response of the structure could be significantly reduced and the structure protected from overall collapse.

2. The innovative idea of casting vertical slits into wall panels so as to increase their ductility and energy dissipation capacity was introduced by Muto in the 1960s.<sup>3,4</sup> He even put

his idea into practice in the design of a number of high-rise seismic resistant buildings in Japan. Subsequently, however, apart from a few experimental studies,<sup>5,6</sup> very little further research work on the effects of adding vertical slits has been carried out. The slit shear wall system proposed by the Authors is not the same as that developed by Muto, albeit there are some similarities in the structural concept. Muto's slit shear walls are really concrete infilled steel frame structures with vertical slits cast within the infilled wall panels. Therefore, to be more precise, Muto's slit shear walls are infilled frames.<sup>7,8</sup> In fact, as Muto's slit wall panels maintain their integrity after cracking only when bounded by and connected to a ductile frame, the original slit wall panel concept was designed for infilled steel frame structures only; it is not directly applicable to ordinary reinforced concrete shear walls. On the other hand, the Authors' slit shear wall system is basically a reinforced concrete shear wall with vertical slits cast along the centroidal axis and is therefore not an infilled frame structure. Nevertheless, the idea of casting vertical slits into the walls so that the behaviour including cracking and finally failure of the walls follows certain preferred patterns with the ductility of the wall structures increased is the same as that of Muto. Hence, the slit shear wall system proposed herein may be considered as an extension of Muto's original concept.

3. Since the proposed slit shear wall system is really the limiting case of a coupled shear wall structure with very short connecting beams, its likely behaviour may be inferred to some extent from that of coupled shear walls. The behaviour of coupled shear walls has been studied extensively by many researchers. Theoretical studies have been carried out by Winokur and Gluck,<sup>9</sup> Paulay,<sup>10</sup> Gluck,<sup>11</sup> Elkholy and Robinson,<sup>12</sup> and Nayer and Coull.<sup>13</sup> They developed several elasto-plastic analysis methods for coupled shear walls which either take into account the limited ductility of the connecting beams or allow the ductility requirements of the beams to be evaluated. Experimental studies by means of cyclic tests or even shake table tests have been undertaken by Lybas,<sup>14</sup> Aristizabal-Ochoa,<sup>15,16</sup> and Shiu, Takayanagi and Corley.<sup>17</sup> The results revealed that lightly coupled and heavily coupled wall systems behave quite differently and that, generally, the connecting beams should be

*Proc. Instn Civ. Engrs Structs & Bldgs*, 1994, **104**, Aug., 317–324

*Structural and Building Board Structural Panel Paper 10456*

*Written discussion closes 18 October 1994*

A. K. H. Kwan,  
*Lecturer,  
Department of Civil  
and Structural  
Engineering,  
University of  
Hong Kong*

Y. K. Cheung,  
*Professor,  
Department of Civil  
and Structural  
Engineering,  
University of  
Hong Kong*

X. L. Lu,  
*Visiting Research  
Associate,  
Department of Civil  
and Structural  
Engineering,  
University of  
Hong Kong*

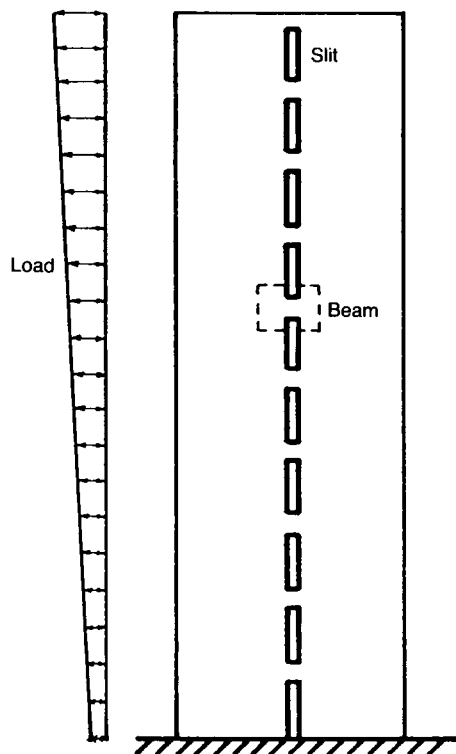


Fig. 1. Typical slit shear wall structure

designed to yield before the walls fail so that their energy dissipation capacity is utilized before the walls are subjected to high ductility demand.

4. All the above studies indicated that the connecting beams have great influence on the overall behaviour of coupled shear wall structures. Paulay<sup>18-20</sup> has studied connecting beams with span/depth ratios ranging from 1.0 to 2.0 and found that connecting beams with such small span/depth ratios behave very differently from the slender beams in beam-column frame structures. Fang<sup>21</sup> has also carried out a series of tests on connecting beams with different amounts of reinforcement. After the investigation, she recommended that to ensure ductile failure, the use of a large amount of longitudinal reinforcement in a beam should be avoided. As shown in Fig. 1, the connecting beams in slit shear walls are even shorter than those in ordinary coupled shear walls. In fact, they are so short that they may

be more appropriately described as thin slices of reinforced concrete acting as shear transfer interfaces.<sup>22,23</sup> Hence, their behaviour is expected to be different, and separate studies are considered necessary. In the study presented herein, two series of shear tests on connecting beams with span/depth ratios ranging from 0.05 to 0.20 and with various amounts of reinforcement were carried out. The first series of tests was to investigate the monotonic load behaviour of the beams, while the second series was to investigate the cyclic load behaviour. As the results of the monotonic shear tests have been reported in reference 1, this Paper concentrates on the results of the cyclic shear tests.

### Test programme

5. Altogether, 24 beam specimens have been constructed and tested. Twelve of the specimens were tested under monotonic shear load and the other twelve were tested under cyclic shear load. In addition to the type of loading, the other variables included in the study are the span/depth ratio of the connecting beam and the area of main reinforcement in the beam. The test program is set out in Table 1. In the table, specimens with designations ending with M were subjected to monotonic shear load, while specimens with designations ending with C were subjected to cyclic shear load. For each set of model parameters, three identical specimens were tested under each type of loading in order to check the repeatability of the test results.

6. Details of the specimens are shown in Fig. 2. All specimens were constructed of the same materials. In particular, specimens with the same set of model parameters, whether for monotonic or cyclic shear tests, were cast at the same time using the same batch of concrete so that their test results may be compared directly. The concrete used has a mean cube strength of 35.5 MPa, while the reinforcements used are mild steel bars with yield strength of 342 MPa. Other details of the test specimens have been given in reference 1.

7. Figure 3 shows the set-up of the tests. Basically, the beam specimen was erected vertically, with one end fixed on to the support, and the shear load was applied horizontally to the other end of the specimen through an electronically controlled hydraulic actuator capable of acting in both the forward and backward directions to produce compression and tension loads. The same set-up was used throughout for the monotonic and cyclic shear tests. Compression load from the actuator was transmitted to the specimen directly by acting against the specimen, while tension load from the actuator was transmitted through steel tie rods tightly connecting the specimen to the actuator, as shown in Fig. 3. The loading procedure for the cyclic tests was as depicted in Fig. 4, where the peak loads at each load cycle were as listed in

Table 1. Testing program

| Specimen series | Depth of beam: mm | Reinforcement         |              | Number of specimens |              |
|-----------------|-------------------|-----------------------|--------------|---------------------|--------------|
|                 |                   | Area: mm <sup>2</sup> | % of section | Monotonic tests     | Cyclic tests |
| IS-5M, IS-5C    | 50                | 113.1                 | 3.02         | 3                   | 3            |
| IS-10M, IS-10C  | 100               | 113.1                 | 1.51         | 3                   | 3            |
| IS-15M, IS-15C  | 150               | 169.6                 | 1.51         | 3                   | 3            |
| IS-20M, IS-20C  | 200               | 169.6                 | 1.13         | 3                   | 3            |

Table 2. Instrumentation for measurement of deflection and strain has been described in reference 1.

**Results of monotonic shear tests**

8. The detailed results of the monotonic shear tests have been given in reference 1. Herein, only a brief summary of the test results and some additional information on ductility of the beams are presented. The main results of the monotonic shear tests are listed in Table 3. They are the averaged results of the three identical specimens in each specimen series. It can be seen that the beams generally started to crack at about 1/5 to 1/3 of their respective failure loads, while the failure load increased with both the depth of the beam and the amount of longitudinal reinforcement in the beam.

9. In each beam specimen, two major cracks were produced. The cracks originated at the beam-wall joints on the tension sides of the joints and extended into the walls at approximately 50–70° to the beam axis, resulting in the formation of a diagonal compression strut between the two parallel cracks in each beam specimen. The transverse component of the diagonal compression provided the shear resistance of the beams while the longitudinal component tended to push the walls apart and, as a result, all the reinforcement was subjected to tension after the beams cracked. The specimens finally failed when the diagonal compression struts were crushed. The failure mechanism is very similar to that described by Mattock<sup>22,23</sup> for shear transfer interfaces. Moreover, an analysis in reference 1 showed that the failure loads of the connecting beams may be evaluated by using Mattock's shear strength equation for shear transfer interfaces.

10. The ductility of the connecting beams is evaluated in terms of their ductility factors defined as the ratios of the deflection at failure (deflection at peak load) to the corresponding deflection when the steel reinforcement started to yield. The last column of Table 3 depicts the ductility factors so determined. Since the rebars in IS-5M did not yield even up to failure, there is no ductility factor available for this specimen series. The average ductility factors of specimen series IS-10M, IS-15M and IS-20M are 2.79, 2.05 and 2.75 respectively, indicating that very short connecting beams can still possess some ductility, provided that the steel reinforcement yields before failure. Comparing the reinforcement ratios of the specimens, it can be seen that the yielding or otherwise of the reinforcement is dependent on the amount of reinforcement provided. When the amount of reinforcement is large as in specimen series IS-5M, the reinforcement would not yield, and when the amount of reinforcement is small as in the other specimens, the reinforcement would yield before

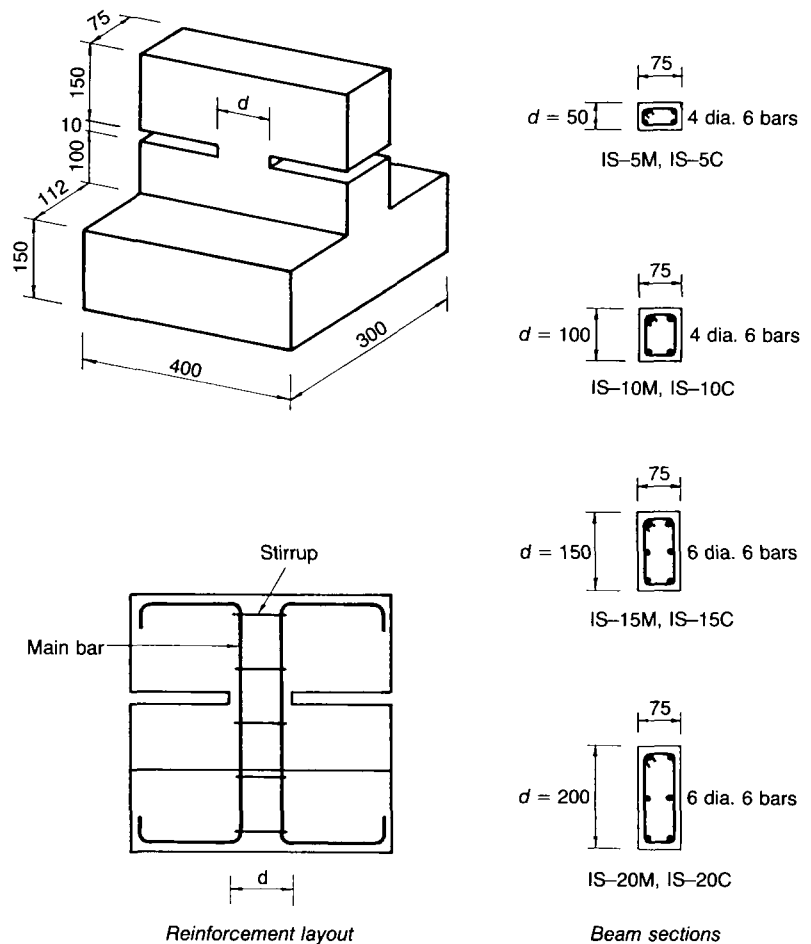


Fig. 2. Details of test specimens: all dimensions in mm

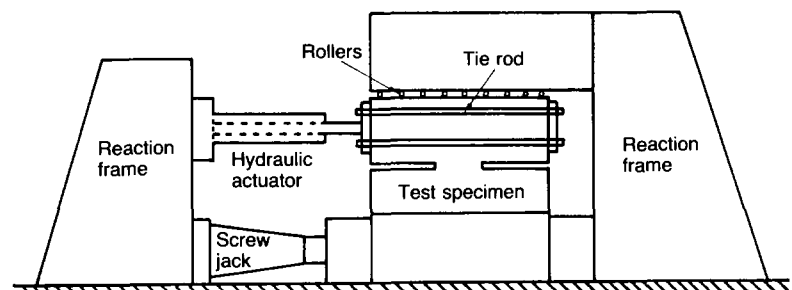


Fig. 3. Test set-up

Table 2. Loading procedure for cyclic shear tests

| Specimen series | $P_1$ : kN | $P_2$ : kN | $P_3$ : kN | $P_4$ : kN | $P_5$ : kN | $P_6$ : kN | $P_7$ : kN | $P_8$ : kN |
|-----------------|------------|------------|------------|------------|------------|------------|------------|------------|
| IS-5C           | 5          | 10         | 15         | 20         | 25         | 30         | 40         | 50         |
| IS-10C          | 5          | 10         | 15         | 20         | 25         | 35         | 50         | 65         |
| IS-15C          | 5          | 10         | 15         | 20         | 30         | 50         | 75         | 90         |
| IS-20C          | 5          | 10         | 15         | 25         | 40         | 60         | 90         | 100        |

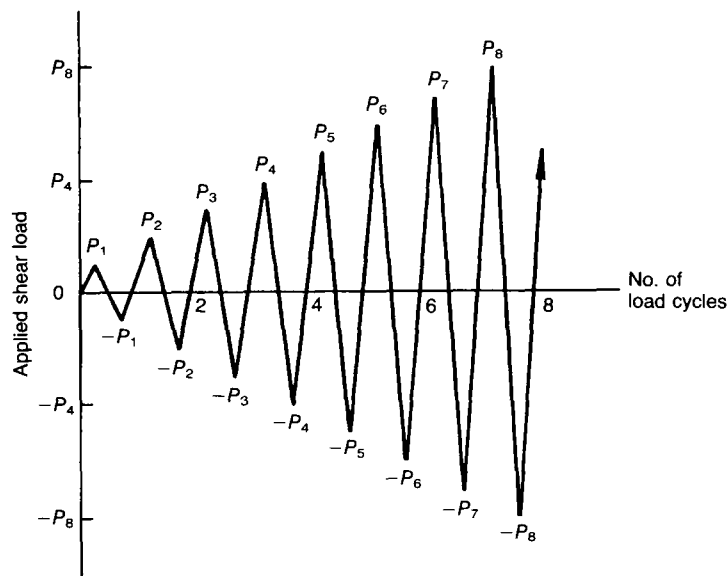


Fig. 4. Loading procedure for cyclic shear tests

failure. In fact, evaluation of the shear strength of the connecting beams according to Mattock's shear transfer theory in reference 22 revealed that the shear failure of IS-5M was governed by concrete crushing while the shear failure of the other specimens was governed by steel yielding. To ensure ductile failure, it is recommended that the beams should be designed such that

shear failure is governed by steel yielding rather than concrete crushing. Using Mattock's shear strength equation, it can be shown that for the steel reinforcement to yield before failure, the total amount of longitudinal reinforcement provided, expressed as a percentage of the beam section area, should not exceed 2.0% when mild steel is used or 1.2% when high yield steel is used.

### Results of cyclic shear tests

11. The load-deflection curves of the four specimen series are plotted in Fig. 5, and the other main results of the cyclic shear tests are tabulated in Table 4. It was generally observed that in the first one or two cycles, before any cracks appeared, the load-deflection curves were very steep and their shapes were more or less the same as those of the initial portions of respective monotonic load-deflection curves. As shown in Table 4, the cracking loads were also approximately the same as those under monotonic load. After the onset of cracks, however, the shear stiffness gradually decreased and the load-deflection curves became more hysteretic. At the cycle shortly before failure, the deflection increased rapidly, resulting in substantial loss of shear stiffness until failure occurred.

12. The crack patterns of the beam specimens after the completion of the cyclic shear tests are shown in Fig. 6. It can be seen that the crack patterns are generally composed of two sets of parallel cracks, each produced by the applied shear load in the forward or backward direction respectively. The two sets of cracks opened and closed alternately as the direction of shear load was reversed. Initially, corresponding to each direction of shear load, only two major cracks originating at the beam-wall joints at the tension sides of the joints were produced as in the monotonically tested beam specimens. However, as the number of load cycles increased, more diagonal cracks, which ran roughly parallel to the initial cracks, appeared. As a result, the cracks produced by cyclic shear load were more numerous than those produced by monotonic shear load. Eventually, a cross-net of cracks was produced in each specimen. In between the two sets of parallel cracks, two sets of diagonal compression struts, each resisting the applied shear load in one direction, were formed. During failure, one set of cracks widened and the diagonal compression struts in between that set of parallel cracks crushed, leading to extensive spalling of the concrete. Relatively speaking, the extents of concrete crushing and spalling were much larger than those in beam specimens tested under monotonic shear load.

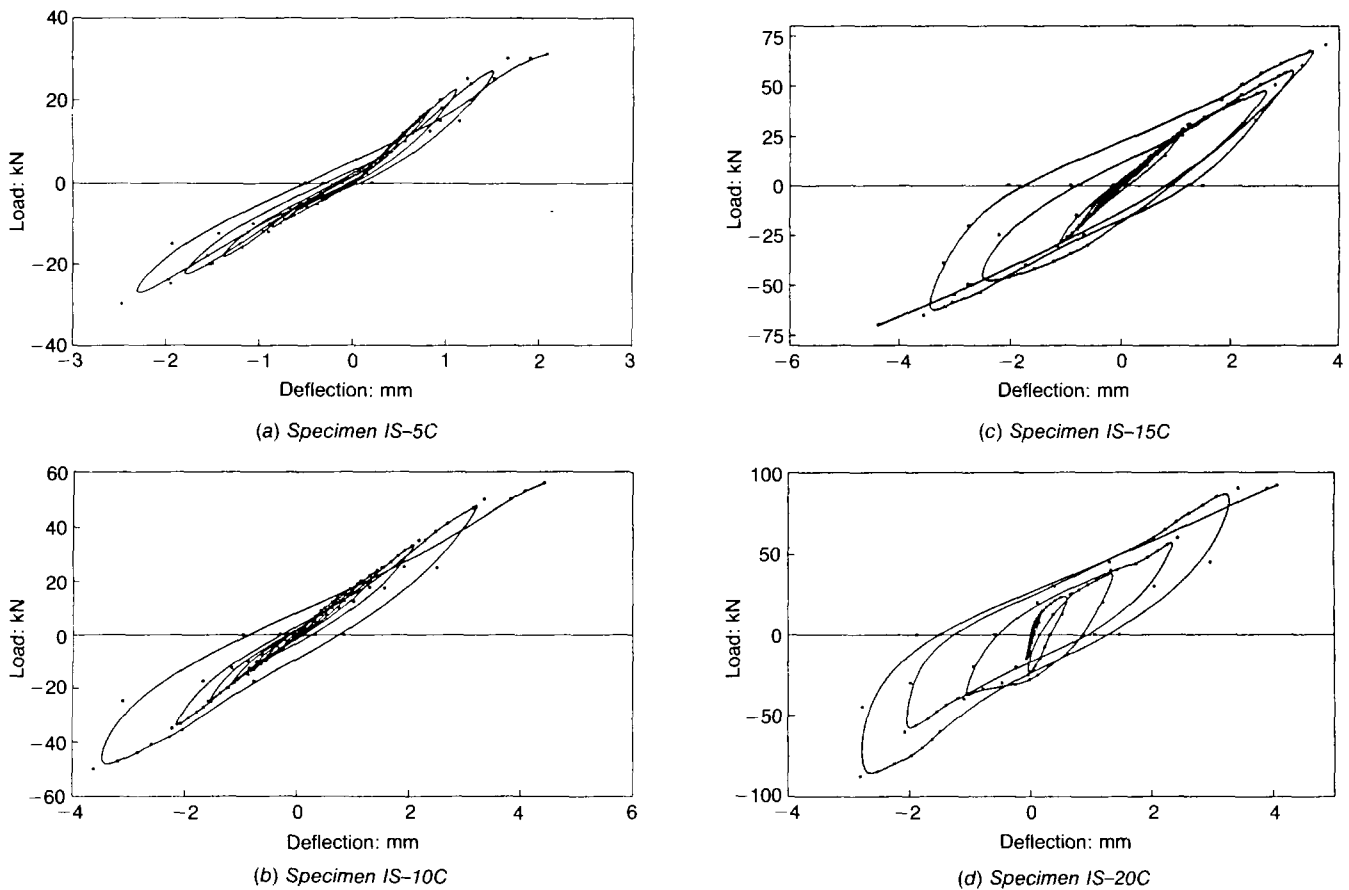
13. The strain conditions of the longitudinal steel reinforcement throughout the cyclic shear tests are studied in the following. During the

Table 3. Results of monotonic shear tests

| Specimen series | Initial stiffness: kN/mm | Cracking load: kN | Failure load: kN | Deflection at failure: mm | Ductility factor |
|-----------------|--------------------------|-------------------|------------------|---------------------------|------------------|
| IS-5M           | 260                      | 12.68             | 39.97            | 1.00                      | —                |
| IS-10M          | 358                      | 13.04             | 63.24            | 1.71                      | 2.79             |
| IS-15M          | 465                      | 16.39             | 74.79            | 1.84                      | 2.05             |
| IS-20M          | 567                      | 13.75             | 87.60            | 3.11                      | 2.75             |

Table 4. Results of cyclic shear tests

| Specimen series | Cracking load: kN | Yielding load: kN | Failure load: kN | Deflection at failure: mm | Ductility factor |
|-----------------|-------------------|-------------------|------------------|---------------------------|------------------|
| IS-5C           | 10.01             | —                 | 28.18            | 2.19                      | —                |
|                 | 9.91              | —                 | 35.94            | 2.68                      | —                |
|                 | 9.97              | —                 | 31.01            | 2.35                      | —                |
| IS-10C          | 15.00             | 33.01             | 60.94            | 4.33                      | 7.06             |
|                 | 10.05             | 22.13             | 53.11            | 4.03                      | 6.58             |
|                 | 10.07             | 25.31             | 55.93            | 3.16                      | 5.16             |
| IS-15C          | 10.05             | 41.95             | 69.86            | 4.39                      | 4.89             |
|                 | 15.03             | 45.05             | 70.24            | 3.75                      | 4.18             |
|                 | 15.07             | 37.46             | 69.91            | 3.50                      | 3.90             |
| IS-20C          | 15.08             | 64.95             | 82.72            | 4.05                      | 3.58             |
|                 | 15.02             | 60.08             | 71.95            | 3.50                      | 3.09             |
|                 | 10.10             | 49.99             | 78.99            | 4.00                      | 3.54             |



first two cycles, before the specimens cracked, the distribution of axial strain in the longitudinal reinforcement was consistent with the contraflexural bending moment distribution in the beams: i.e. at each beam-wall joint, one of the bars was in tension while the other was in compression, as in beam specimens subjected to monotonic shear load. Furthermore, the steel strain changed from tension to compression or from compression to tension alternately as the direction of shear load was reversed. After cracking, however, all longitudinal reinforcement gradually became in tension at all times irrespective of the direction of the applied shear load. This observation agrees with that of Paulay<sup>19</sup> on the cyclic behaviour of connecting beams with span/depth ratios ranging from 1.0 to 2.0.

14. It was also observed after completion of the tests, when spalling of concrete rendered the steel reinforcement to be exposed, that the longitudinal bars were bent like dowel bars during failure of the beams (Fig. 7). Moreover, after being bent, the middle portions of the longitudinal bars were inclined at fairly large angles of approximately 45° to the original beam axis in all beam specimens. It is likely, therefore, that the dowel action and the transverse component of the axial tension in the reinforcement had contributed significantly to

the residual shear capacity of the beams after the peak resistance had been attained. As none of the reinforcement bars was broken after the cyclic tests, the steel bars should be able to withstand some more cycles of shear load reversal without breakage. Such residual shear capacity might be important in preventing catastrophic collapse of the overall structure. In order to make sure that the longitudinal reinforcement can fully develop such potential, careful detailing is necessary. Generally, generous anchorage should be provided to the longi-

Fig. 5. Load-deflection curves of cyclically tested specimens

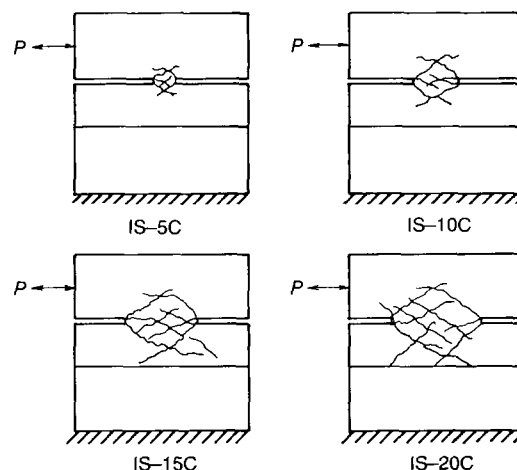


Fig. 6. Crack patterns of cyclically tested specimens

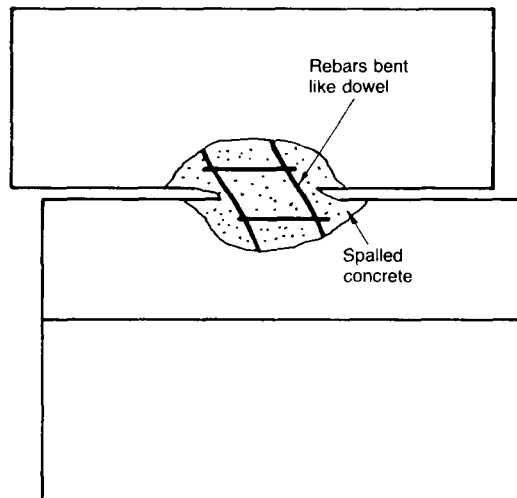


Fig. 7. Specimen IS-10C after failure

tudinal bars and no splicing of the bars should be allowed within the span lengths of the beams.

15. From the load-deflection curves, it is evident that there was substantial stiffness degradation as the beam specimens were tested to ultimate failure. During the first one or two cycles, before the specimens cracked, there was little change in shear stiffness. However, as soon as cracks appeared, the effective stiffness of the specimens, defined as the secant stiffness at peak load of the cycle being referred to, decreased very rapidly. For instance, at the fourth cycle, when all specimens had cracked, the effective stiffness of the specimens decreased to approximately 20% of their respective initial stiffness. Further significant degradation occurred when the specimens were loaded to failure. At the last cycle, the effective stiffness of the specimens decreased to 16 kN/mm, 18 kN/mm, 20 kN/mm and 24 kN/mm for specimens IS-5C, IS-10C, IS-15C and IS-20C respectively, which were only about 5% of their respective initial stiffness. The rapid stiffness degradation of the connecting beams as the beams crack significantly reduces the lateral stiffness and hence the natural frequency of the slit shear wall system, and, if the seismic energy lies mostly in the high frequency range, this can detune the structural system to avoid

dynamic amplification due to resonance. Furthermore, the stiffness degradation also helps to reduce the degree of over-coupling which, as many researchers have found,<sup>14-17</sup> would cause the walls to be severely damaged at the junctions with their foundations before the energy dissipation capacity of the beams could be utilized.

16. However, although the shear stiffness of the beams degraded fairly rapidly and substantially, there was relatively little reduction in shear strength, as shown in Table 5 where the average failure loads of the cyclically tested specimens are compared with those of monotonically tested specimens. Generally speaking, the failure loads of the cyclically tested specimens were lower than those of corresponding monotonically tested counterparts by only 10-20%; i.e. after the high intensity load reversals, the short connecting beams still maintained shear strength equal to 0.8-0.9 of their respective shear strength under monotonic shear load. It is interesting to note at this point that similar results have been obtained by Paulay<sup>19</sup> on the cyclic shear strength of connecting beams with span/depth ratios of 1.0-2.0 and by Mattock<sup>23</sup> on the cyclic shear strength of shear transfer interfaces. Hence, it may be said that the very short connecting beams were rather 'tough'. This 'toughness', or in other words, capability of the beams to maintain substantial portions of their strength after being subjected to high intensity load reversals, is a highly desirable quality for connecting beams in coupled shear wall structures, for if the beams are not tough enough, they may fail prematurely without contributing much to the lateral stability of the wall structure. On the other hand, since the shear loads on the connecting beams are always cyclic when the coupled wall structure is subjected to seismic excitation, the shear strength of the beams for earthquake design calculations should not be taken as larger than 0.8 of their respective monotonic shear strength.

17. The deflection ductility of the cyclically tested specimens are evaluated in terms of their ductility factors which are defined in a similar way as for the monotonically test specimens, namely as the ratios of the deflection at failure (deflection at peak load during the last cycle) to the corresponding deflection when the steel reinforcement started to yield, and are given in the last column of Table 4. Since the rebars in IS-5C did not yield, there is no ductility factor available for this specimen series. The average ductility factors for specimen series IS-10C, IS-15C and IS-20C are 6.27, 4.32 and 3.40 respectively. They are generally higher than those of the monotonically tested specimens but are still somewhat lower than those obtained by Paulay.<sup>20</sup> Hence a major problem with the development of the proposed slit shear wall

Table 5. Comparison of monotonic and cyclic shear strength

| Specimen series | Monotonic shear strength: kN | Cyclic shear strength: kN | Ratio of cyclic strength to monotonic strength |
|-----------------|------------------------------|---------------------------|--|
| IS-5M, IS-5C    | 39.97                        | 31.71                     | 0.79   |
| IS-10M, IS-10C  | 63.24                        | 56.66                     | 0.90   |
| IS-15M, IS-15C  | 74.79                        | 70.00                     | 0.94   |
| IS-20M, IS-20C  | 87.60                        | 77.89                     | 0.89   |

system could be the relatively low ductility of the short connecting beams. Further studies using other reinforcement details, e.g. diagonal reinforcements, that could possibly improve the ductility are recommended. It should also be borne in mind that the ductility factor is dependent on the test conditions and how it is defined. Theoretically, when the ductility of a structural member is being evaluated, the entire range of load–deflection curves, including the descending part, should be taken into account. With the present definition of ductility factor used, as only the deflection at peak load is taken to evaluate the ductility, the residual strength of the structural member after peak load is reached is totally ignored and, as a result, a complete picture of the ductility performance of the member is not obtained. The Authors are of the opinion that a better way of defining the ductility factor is to use the deflection when the load drops, after reaching the peak, to 0.8 of the maximum load instead of the deflection at peak load in the ductility evaluation. However, this would require the tests to be carried out under displacement control. It is recommended, therefore, that when further tests are to be carried out, serious considerations should be given to the possibility of performing the tests under displacement control so that the entire load–deflection curves may be obtained for ductility evaluation.

18. The damping ratio defined by Jacobsen<sup>24</sup> is used in the following to study the damping characteristics of the beam specimens. According to the definition, the damping ratio  $\zeta$  in any loading cycle is given by

$$\zeta = \frac{1}{2\pi} \frac{A_h}{A_s} \quad (1)$$

where  $A_h$  is the area within the hysteresis loop, and  $A_s$  is the area under the skeleton curve. The average values of the damping ratios for each test specimen series are tabulated in Table 6. It can be seen from the results that during the first two cycles, before the specimens cracked, the damping ratios were rather small as for many other elastic structures. Starting at the third cycle, when the load–deflection curves became more hysteretic, the damping ratios gradually increased until at the cycle immediately before failure, the damping ratios were 0.08, 0.12, 0.15 and 0.17 for specimens IS-5C, IS-10C, IS-15C and IS-20C respectively. Among the different specimens, the damping ratios of specimens IS-5C remained relatively small even up to failure. As the rebars in these specimens did not yield even during failure, a probable reason for their low damping ratios was their lack of energy dissipation by means of steel yielding. The damping ratios of the other specimens, namely IS-10C, IS-15C and IS-20C, agree fairly well with those obtained by Mattock<sup>23</sup> for shear transfer interfaces.

Table 6. Damping ratios of the cylindrically tested specimens

| No. of cycle | Damping ratios at each cycle |        |        |        |
|--------------|------------------------------|--------|--------|--------|
|              | IS-5C                        | IS-10C | IS-15C | IS-20C |
| 1            | 0.04                         | 0.04   | 0.05   | 0.06   |
| 2            | 0.04                         | 0.05   | 0.05   | 0.07   |
| 3            | 0.04                         | 0.05   | 0.06   | 0.08   |
| 4            | 0.05                         | 0.06   | 0.08   | 0.11   |
| 5            | 0.06                         | 0.07   | 0.12   | 0.14   |
| 6            | 0.08                         | 0.09   | 0.15   | 0.17   |
| 7            | Failed                       | 0.12   | Failed | Failed |
| 8            | Failed                       | Failed | Failed | Failed |

### Conclusions

19. In addition to the monotonic shear tests which have been reported previously, cyclic shear tests on simulated connecting beams in slit shear walls have been carried out. From the cyclic shear tests, the following conclusions may be drawn.

20. Under cyclic shear load, the connecting beams crack at more or less the same loads as in the monotonic loading case. In each beam, two sets of parallel cracks with diagonal compression struts formed in between would be produced. The transverse component of the diagonal compression resists the shear load while the longitudinal component causes the longitudinal rebars to be in tension at all times irrespective of the loading direction. Peak load would be reached when the diagonal struts fail in compression and after that, the rebars would bend like dowel bars and continue to contribute some residual shear capacity.

21. The connecting beams show fairly rapid stiffness degradation as cracks appear, and when they are close to shear failure, their effective stiffness may drop to only about 5% of their respective initial stiffness. Nevertheless, the corresponding reductions in strength are relatively small; after high intensity load reversals, the connecting beams can still maintain 0.8–0.9 of their respective monotonic shear strength. The rapid stiffness degradation and high toughness of the connecting beams are highly desirable because they would allow the energy dissipation capacity of the beams to be fully utilized before the walls fail.

22. The ductility factors of the connecting beams are higher under cyclic load than under monotonic load but are still apparently quite low. Further investigations on how to improve the ductility of the beams are recommended. It is also suggested that any further tests should be carried out under displacement control so that the entire load–deflection curve, including the descending part, may be obtained for ductility evaluation.

23. Before cracking, the damping ratios of the connecting beams are quite low, but after



cracking, the damping ratios would gradually increase and the connecting beams become more effective as energy dissipation devices. Provided that the rebars yield before failure, the damping ratios of the beams would increase to about 0.1–0.2 before failure.

24. Connecting beams whose rebars do not yield before failure are less ductile, less tough, and have smaller damping capacity. For the rebars to yield before failure, the amount of reinforcement provided should not exceed 2.0% when mild steel is used or 1.2% when high yield steel is used. Moreover, in order to ensure that the rebars can fully develop their strength and ductility potentials, generous anchorage should be provided and no splicing of rebars should be allowed.

### Acknowledgement

25. The financial support of the Croucher Foundation for the research work presented herein is gratefully acknowledged.

### References

1. CHUENG Y. K., KWAN A. K. H. and LU X. L. Shear tests on simulated connecting beams in reinforced concrete slit shear walls. *Proc. Instn Civ. Engrs Structs & Bldgs*, **99**, Nov., 1993, 481–488.
2. KWAN A. K. H., LU X. L. and CHEUNG Y. K. Elastic analysis of slitted shear walls. *Int. J. Structs*, 1993, **13**, No. 2, Dec., 75–92.
3. MUTO K. Earthquake resistant design of 36-storied Kasumigaseki Building. *Proc. 4th World Conf. on Earthquake Engng*, Santiago de Chile, 1969, J4: 15–33.
4. MUTO K., OHMORI N. and TAKAHASHI T. A study on reinforced concrete slitted shear walls for high-rise buildings. *Proc. 5th World Conf. on Earthquake Engineering*, Rome, 1973, 1135–1138.
5. SHEU M. S., LO P. T. and CHEN Y. S. Comparison of slitted and non-slitted r. c. shear walls with boundary elements under horizontal forces. *Seismic Engineering: Research and Practice, Proc. Structural Congr. '89*, San Francisco, 1989, 566–575.
6. DING D. J. Experimental studies on aseismic control of building structures. *Proc. 2nd Int. Conf. on Highrise Buildings*, Nanjing, 1992, 61–80.
7. KLINGER R. E. and BERTERO V. V. Earthquake resistance of infilled frames. *J. Struct. Div. Am. Soc. Civ. Engrs*, 1978, **104**, No. ST6, June, 973–989.
8. LIAUW T. C. and KWAN K. H. Unified plastic analysis for infilled frames. *J. Struct. Engng. Am. Soc. Civ. Engrs*, 1985, **111**, No. 7, July, 1427–1428.
9. WINOKUR A. and GLUCK J. Ultimate strength analysis of coupled shear walls. *J. Am. Concr. Inst.*, 1968, **65**, No. 12, Dec., 1029–1035.
10. PAULAY T. An elasto-plastic analysis of coupled shear walls. *J. Am. Concr. Inst.*, 1970, **67**, No. 11, Nov., 915–922.
11. GLUCK J. Elasto-plastic analysis of coupled shear walls. *J. Struct. Div. Am. Soc. Civ. Engrs*, 1973, **99**, No. ST8, Aug., 1743–1760.
12. ELKHOLY I. A. S. and ROBINSON H. An inelastic analysis of coupled shear walls. *Build. Sci.*, 1974, **9**, 1–8.
13. NAYAR K. K. and COULL A. Elastoplastic analysis of coupled shear walls. *J. Struct. Div. Am. Soc. Civ. Engrs*, 1976, **102**, No. ST9, Sept., 1845–1860.
14. LYBAS J. M. Concrete coupled walls: earthquake tests. *J. Struct. Div. Am. Soc. Civ. Engrs*, 1981, **107**, No. ST5, May, 835–855.
15. ARISTIZABAL-OCHOA J. D. Seismic analysis of slender coupled walls. *J. Struct. Engng. Am. Soc. Civ. Engrs*, 1983, **109**, No. 7, July, 1538–1552.
16. ARISTIZABAL-OCHOA J. D. Seismic behaviour of slender coupled wall systems. *J. Struct. Engng. Am. Soc. Civ. Engrs*, 1987, **113**, No. 10, Oct., 2221–2234.
17. SHIU K. N., TAKAYANAGI T. and CORLEY W. G. Seismic behaviour of coupled wall system. *J. Struct. Engng. Am. Soc. Civ. Engrs*, 1984, **110**, No. 5, May, 1051–1066.
18. PAULAY T. Coupling beams of reinforced concrete shear walls. *J. Struct. Div. Am. Soc. Civ. Engrs*, 1971, **97**, No. ST3, Mar., 843–862.
19. PAULAY T. Simulated seismic loading of spandrel beams. *J. Struct. Div. Am. Soc. Civ. Engrs*, 1971, **97**, No. ST9, Sept., 2407–2419.
20. PAULAY T. and SANTHAKUMAR A. R. Ductile behavior of coupled shear walls. *J. Struct. Div. Am. Soc. Civ. Engrs*, 1976, **102**, No. ST1, Jan., 93–108.
21. FANG E. H. Experimental investigation and seismic design of coupling beams in the tall shear wall structures. *Proc. 4th Int. Conf. on Tall Buildings*, Hong Kong and Shanghai, April/May, 1988, **2**, 972–978.
22. MATTOCK A. H. and HAWKINS N. M. Shear transfer in reinforced concrete—recent research. *J. Prestr. Concr. Inst.*, 1972, **17**, No. 2, Mar.–Apr. 55–75.
23. MATTOCK A. H. Cyclic shear transfer and type of interface. *J. Struct. Div. Am. Soc. Civ. Engrs*, 1981, **107**, No. ST10, Oct., 1945–1964.
24. JACOBSEN L. S. Damping in composite structures. *Proc. 2nd World Conf. on Earthquake Engineering*, Tokyo and Kyoto, 1960, **2**, 1029–1044.